EPJ Photovoltaics **7**, 70305 (2016)
www.epj-pv.org
DOI: 10.1051/epjpv/2016005

Fabrication of solar cells based on Cu_2ZnSnS_4 prepared from Cu_2SnS_3 synthesized using a novel chemical procedure

John M. Correa[1], Raúl A. Becerra[2], Asdrubal A. Ramírez[3], and Gerardo Gordillo[4,a]

[1] Department of Mechanical Engineering, Universidad Nacional de Colombia, Bogotá, Colombia
[2] Department of Chemistry, Universidad Nacional de Colombia, Bogotá, Colombia
[3] Department of Chemistry Engineering, Universidad Nacional de Colombia, Bogotá, Colombia
[4] Department of Physics, Universidad Nacional de Colombia, Bogotá, Colombia

Received: 1 July 2016 / Received in final form: 17 September 2016 / Accepted: 26 September 2016

Abstract Solar cells based on kesterite-type Cu_2ZnSnS_4 (CZTS) thin films were fabricated using a chemical route to prepare the CZTS films, consisting in sequential deposition of Cu_2SnS_3 (CTS) and ZnS thin films followed by annealing at 550 °C in nitrogen atmosphere. The CTS compound was prepared in a one-step process using a novel chemical procedure consisting of simultaneous precipitation of Cu_2S and SnS_2 performed by diffusion membranes assisted CBD (chemical bath deposition) technique. Diffusion membranes were used to optimize the kinetic growth through a moderate control of release of metal ions into the work solution. As the conditions for the formation in one step of the Cu_2SnS_3 compound have not yet been reported in literature, special emphasis was put on finding the parameters that allow growing the Cu_2SnS_3 thin films by simultaneous precipitation of Cu_2S and SnS_2. For that, we propose a methodology that includes numerical solution of the equilibrium equations that were established through a study of the chemical equilibrium of the system $SnCl_2$, $Na_3C_6H_5O_7{\cdot}2H_2O$, $CuCl_2$ and $Na_2S_2O_3{\cdot}5H_2O$. The formation of thin films of CTS and CZTS free of secondary phases grown with a stoichiometry close to that corresponding to the Cu_2SnS_3 and Cu_2ZnSnS_4 phases, was verified through measurements of X-ray diffraction (XRD) and Raman spectroscopy. Solar cell with an efficiency of 4.2%, short circuit current of 16.2 mA/cm^2 and open-circuit voltage of 0.49 V was obtained.

1 Introduction

The recent growth of the thin-film Photovoltaic (PV) industry and its high cell efficiencies of 22.3% for $Cu(In,Ga)Se_2$ [1], demonstrate the viability of this as an option for large-scale power generation. However, the limited availability of In, brings some concern that high material expenses restrict the capacity to lower production costs, especially in view of the desired industrial mass production. Cu_2ZnSnS_4 has been considered as the alternative absorber layer to $Cu(In,Ga)Se_2$ due to its optimal direct band gap and earth abundance and environmental friendly constituents [2, 3]. In recent years, great efforts have focused on the preparation of CZTS thin films and exploration of their potential application in thin film solar cells [3–5].

A variety of routes has been undertaken for thin-film deposition. These include vacuum and solution based deposition approaches. In most of these deposition routes, the growth of single phase CZTS films remains the main barrier toward a reliable process. This barrier is attributed to the incompletely understood nature of the Cu-Zn-Sn-S phase diagram [6] and to the volatility upon heating of Sn [7]. Despite these limitations, reasonably successful film deposition and device fabrication have been demonstrated for both vacuum and solution-based deposition approaches. Several groups have reported the fabrication of CZTS thin films using a variety of methods such as sulfurization [8], electrodeposition [9,10] RF sputtering [11] and co-evaporation [2]. Kim et al. achieved a 12,7% efficient $Cu_2ZnSn(Se,S)_4$ device [12] fabricated from CZTSSe films prepared using a hydrazine-based pure solution approach and employing an In_2S_3 /CdS double-emitter on CZTSSe absorbers upon annealing under optimized conditions.

In this work, we use a new procedure to grow Cu_2SnS_3 thin films, which were successfully used as a precursor of Cu_2ZnSnS_4 thin films [13]. This procedure consist of simultaneous precipitation of Cu_2S and SnS_2 performed by diffusion membranes assisted CBD technique. The parameters that allow the growth of Cu_2SnS_3 films by simultaneous precipitation of Cu_2S and SnS_2 were obtained through a numerical solution of the equilibrium equations,

[a] e-mail: ggordillog@unal.edu.co

which were established by means of a study of the chemical equilibrium of the system $SnCl_2$, $Na_3C_6H_5O_7{\cdot}2H_2O$, $CuCl_2$ and $Na_2S_2O_3{\cdot}5H_2O$. It is well known that in a process CBD, the controlled release of ions precursors to the working solution favors the ion by ion growth [14]; therefore we consider that a controlled release of ions achieved by the physical barrier provided by the diffusion membrane favors the growth ion by ion and decreases the cluster growth. In this work we were able to optimize the control of the supply of ions by selecting adequately the porosity of the membranes; this aspect constitutes the main advantage of this method respect to the conventional CBD.

Measurements of XRD and Raman spectroscopy confirmed the formation of the Cu_2SnS_3 compound as well as the Cu_2ZnSnS_4 compound; this latter was obtained by sequential deposition of Cu_2SnS_3 and Zn(S,O) thin films followed by annealing at 550 °C in nitrogen atmosphere. The applicability of the CZTS films grown using the method proposed in this work for photovoltaic devices has been demonstrated using them as absorber layer, in CZTS based solar cells.

2 Experimental

The CBD process has its basis on the controlled precipitation of some material onto the surface of a particular substrate. This precipitation could occur in homogeneous phase (i.e. in the solution), or heterogeneous phase (i.e. in the substrate) [15,16], and the thin film formation takes place when the ionic product exceeds the solubility product.

The synthesis of the Cu_2SnS_3 compound was performed on soda-lime glass substrates following a new route developed in our laboratory, which involves simultaneous precipitation of Cu_2S and SnS_2 into a work solution where the substances react giving rise to the formation of the ternary compound. The co-precipitation of Cu_2S and SnS_2 was done using two spatially separated diffusion membranes of nitrocellulose with porosity of 0.45 μm. The first one contained a solution of $CuCl_2$ as Cu^{2+} ion source and the second one contained a $SnCl_2$ solution, which was complexed with sodium citrate ($Na_3C_3H_5O(COO)_3$) to form the $[SnH_nCit]^{(n-1)}$ complexes; these species diffuse through the membranes into a solution of sodium thiosulfate ($Na_2S_2O_3$) where HS^- ions are formed by hydrolysis. Sodium thiosulfate also acts as a reducing agent of Cu^{2+} ions to generate Cu^+ and as an oxidizing agent of the Sn^{2+} to obtain Sn^{4+}. The co-precipitation of Cu_2S and SnS_2 results in thin films of Cu_2SnS_3 that typically grow at a rate of 15 nm/min. Figure 1 shows a diagram of the system implemented for the synthesis of Cu_2SnS_3 thin films. The system includes a double-wall glass reactor, a magnetic and mechanical agitator of the working solution, membranes and substrate holders fabricated in teflon and indirect heating of the work solution through a hot water flow that circulates between the walls of the reactor; this system also includes a pumping system and an electronic control (PID) of the working solution temperature.

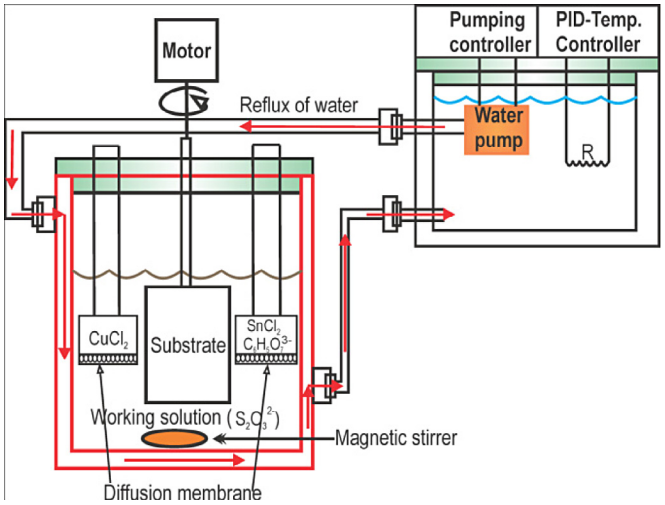

Fig. 1. System implemented for the synthesis of thin films of Cu_2SnS_3, by co-precipitation of Cu_2S and $SnCl_2$, through diffusion membranes.

The possible reaction mechanism for the formation of the Cu_2SnS_3 compound, proposed in this work follows the next steps:

– Formation of HS^- ions according to the following reaction:

$$S_2O_3^{2-} + H_2O \rightleftarrows SO_4^{2-} + HS^- + H^+. \quad (1)$$

– Once formed HS^- ions, free Sn^{4+} is needed in the reaction medium to precipitate of SnS_2; this process occurs in four stages:

i) diffusion of the $[SnH_nCit]^{(n-1)}$ complexes to the solution through the membrane:

$$[SnH_nCit]^{(n-1)}\ \text{membrane} \rightleftarrows [SnH_nCit]^{(n-1)}\ \text{solution} \quad (2)$$

ii) chemical equilibrium between Sn^{2+} ion and the $[SnH_nCit]^{(n-1)}$ complexes:

$$Sn^{2+} + H_nCit^{(n-3)} \rightleftharpoons [SnH_nCit]^{(n-1)} \quad (3)$$

iii) oxidation of ion Sn^{2+} to Sn^{4+} where the thiosulfate works as an oxidizing agent:

$$4Sn^{2+} + S_2O_3{}^{2-} + 8H^+ \rightarrow 4Sn^{4+} + 2HS^- + 3H_2O \quad (4)$$

iv) precipitation of the SnS_2 compound:

$$Sn^{4+} + 2HS^- \rightarrow SnS_2 + 2H^+. \quad (5)$$

– An additional formation of CuS_2 takes place in four steps as follow:

i) diffusion of Cu^{2+} ions to the solution through the membrane:

$$Cu^{2+}\ \text{membrane} \rightleftarrows Cu^{2+}\ \text{solution} \quad (6)$$

ii) formation of the $[Cu(S_2O_3)_n]^{(1-2n)}$ complexes:

$$Cu^+ + nS_2O_3^{2-} \rightleftharpoons [Cu\,(S_2O_3)_n]^{(1-2n)} \quad (7)$$

iii) reduction of Cu^{2+} ion to Cu^+ using thiosulphate as a reducing agent:

$$2Cu^{2+} + 2{S_2O_3}^{2-} \rightleftharpoons 2Cu^+ + S_4O_6^{2-} \quad (8)$$

iv) precipitation of Cu_2S:

$$2Cu^+ + HS^- \rightarrow Cu_2S + H^+. \quad (9)$$

– After the formation of SnS_2 and Cu_2S, the compounds react in solution to form the ternary compound Cu_2SnS_3 according to the following reaction:

$$SnS_2 + Cu_2S \rightarrow Cu_2SnS_3. \quad (10)$$

In the whole process the diffusion through the membranes favors the ion by ion growth and decreases the cluster growth, because of the physical barrier provided by the membrane.

The preparation of Cu_2ZnSnS_4 films was achieved by sequential deposition of Cu_2SnS_3 and Zn(S,O) films followed by annealing at 550 °C in nitrogen atmosphere. The synthesis of the Cu_2SnS_3 films was performed using the procedure described above and the Zn(S,O) films were deposited by conventional CBD method using a solution containing thiourea (CSN_2H_4) as source of HS^- ions, zinc acetate ($ZnC_4H_6O_4{\cdot}2H_2O$) as source of Zn^{2+} ions, sodium citrate ($Na_3C_6H_5O_7{\cdot}2H_2O$) as complexing agent and ammonia (NH_3) for pH adjustment. The following chemical bath composition leaded to good results: [zinc acetate] = 150 mM; [thiourea] = 150 mM; [sodium citrate] = 30 mM. During the deposition, the bath temperature was maintained at 80 °C and the solution pH around 10.0. The annealing was done with a furnace placed inside a chamber, which was previously evacuated up to reaching a vacuum of 5×10^{-3} mB and then nitrogen was introduced up to reaching a pressure of 10 mB. Subsequently de CTS/Zn(S,O) system was heated at 550 °C without sulfur addition. Single phase Cu_2ZnSnS_4thin films were achieved using a thickness ratio of CTS/Zn(S,O) of about 2.6. For solar cells fabrication, we used typically 2.5 μm thick CZTS films (CTS layer 1.8 μm thick and ZnS layer 0.7 μm thick). Taking into account that both the layer of Cu_2SnS_3 as the Zn(S,O) grow at a rate of about 15 nm/min, the time that takes the growth of a CZTS layer of 2.5 μm is around 2.7 h.

The characterization involved X-ray diffraction on a Shimadzu-6000 diffractometer and Raman spectroscopy on a Horiba Jobin Yvon micro-Raman Spectrometer LabRamHR in backscattering configuration with a laser of 780 nm, 20 mW focused with a 50X objective. The resistivity of the CZTS films was done using the four probe method with contacts placed on the surface of the sample and the film thickness was determined using a Veeco Dektak 150 surface profiler. The SEM images were carried out with a Fei Quant 200 electron microscope in high vacuum mode using an Everhart-Thorney detector.

3 Theoretical determination of synthesis parameters of the Cu_2SnS_3 compound

In this work, special emphasis was made on the development of a route of synthesis of Cu_2SnS_3 thin films grown in one-stage process, by means of the mechanism ion to ion; this was carried out using a new procedure consisting in supplying simultaneously the precursor solutions of Cu_2S and SnS_2 to a solution of sodium thiosulfate, making them pass across membranes of nitrocellulose.

At the beginning we find difficulties because the conditions to grow in one step the Cu_2SnS_3 compound have not yet been reported in literature; however, prior to obtaining experimental conditions for its preparation, we overcome this difficulty finding parameters of synthesis of reference for the growth of Cu_2SnS_3 by means of theoretical simulation of the formation of this compound. For that, we proposed a methodology that is described next.

Initially the different equilibria of the system $SnCl_2$, $Na_3C_6H_5O_7{\cdot}2H_2O$, $CuCl_2$ and $Na_2S_2O_3{\cdot}5H_2O$ were studied. The study was performed establishing the possible aqueous equilibrium presented by the reagents used, a standard initial concentration and a temperature range.

The main equilibria reported for this system are the following [17–20]:

$$S_2O_3^{2-} + H_2O \rightleftharpoons SO_4^{2-} + S^{2-} + 2H^+ \quad (11)$$

$$2Cu^{2+} + 2{S_2O_3}^{2-} \rightleftharpoons 2Cu^+ + {S_4O_6}^{2-} \quad (12)$$

$$Sn^{2+} + H_nCit^{(n-3)} \rightleftharpoons [SnH_nCit]^{(n-1)} \quad (13)$$

$$4Sn^{2+} + {S_2O_3}^{2-} + 8H^+ \rightarrow 4Sn^{4+} + 2HS^- + 3H_2O \quad (14)$$

$$2Cu^+ + S^{2-} \rightarrow Cu_2S \quad (15)$$

$$Sn^{4+} + 2S^{2-} \rightarrow SnS_2. \quad (16)$$

Once established all the possible chemical equilibria, a numerical simulation of the equilibrium state for the system was performed with the help of the Visual MINTEQ 3.0 package, supported on the program MINTEQA2, using values of the equilibrium constant (K_{eq}) and of the standard reaction enthalpy change ($\Delta_r H°$) for each reaction. Additional to the Visual MINTEQ 3.0 package the simulations were carried out using the simple Davies activity correction model, considering that the range of concentrations used in the study is low. To see the effect of the temperature on the chemical equilibriums, the program uses the Van't Hoff equation:

$$\frac{d\,(\ln K_{eq})}{dT} = \frac{\Delta_r H°}{RT^2}. \quad (17)$$

It is assumed that $\Delta_r H°$ has no dependence with the temperature, which is a good approximation keeping in mind that the range of temperatures studied is low (60–80 °C) and that these values are close to the standard temperature.

To obtain the concentration of reagents required to grow Cu_2SnS_3 thin films as a function of the initial concentration of metal ions at various temperatures, the entire

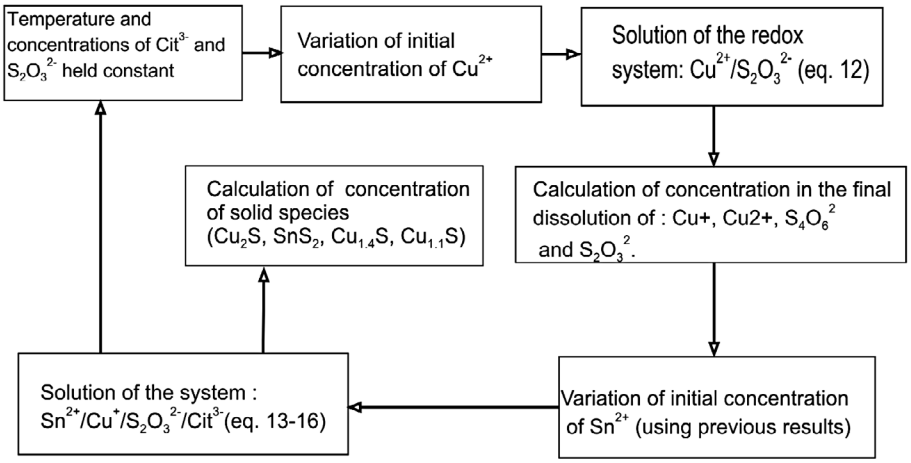

Fig. 2. Flow diagram indicating the methodology followed for the thermodynamic simulation of growth conditions of Cu_2SnS_3 thin films.

system represented by equations (11) to (16), was solved using a methodology that is outlined in the flow diagram shown in Figure 2.

The equilibrium equation is always solved keeping constant the concentrations of $Na_2S_2O_3$ and $Na_3C_6H_5O_7$ at 230 mM and 180 mM respectively; the concentration of $Na_2S_2O_3$ is maintained at 250 mM to ensure an excess of $S_2O_3^{2-}$, resulting in a concentration of Cu^{2+} and Sn^{2+} enough for the formation of of Cu_2S and SnS_2 throughout the process. Otherwise there form oxides of Cu and Sn that can precipitate in the film. The concentration of $Na_3C_6H_5O_7$ is maintained in 180 mM to prevent the formation of SnO.

Calculations are started varying the concentration of $CuCl_2$ between 2 and 80 mM, maintaining constant the concentration of $SnCl_2$ at 20 mM and solution temperature at 60 °C. Subsequently the concentration of $SnCl_2$ is varied between 1 and 60 mM keeping constant the concentration of $CuCl_2$ at 40 mM. Finally the temperature is varied between 60 and 80 °C maintaining constant the concentrations of $SnCl_2$ and $CuCl_2$ in 20 and 40 mM respectively.

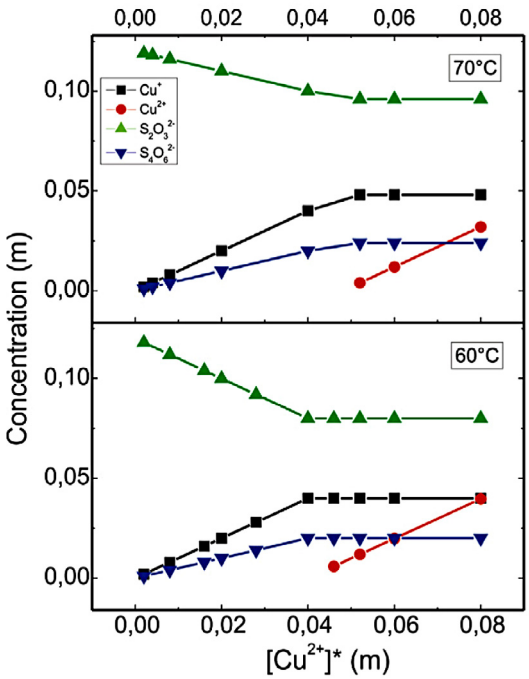

Fig. 3. Variation of the concentration of species produced during the reduction of Cu^{2+} with thiosulfate at different temperatures as a function of the initial concentration of Cu^{2+}.

4 Results and discussion

4.1 Cu^{2+} reduction

Results obtained from the theoretical simulation of the processes occurring during the reduction of Cu^{2+} with thiosulfate at different temperatures are shown in Figure 3. In particular, the concentration of the main species produced (Cu^+, $S_4O_6^-$, $S_2O_3^{2-}$) are plotted as function of the initial concentration of Cu^{2+}($[Cu^{2+}]^*$). It can be observed that both Cu^+ concentration as the $S_4O_6^-$ concentration increase linearly with increasing concentration of Cu^{2+}, while the concentration of $S_2O_3^{2-}$ decreases linearly with increasing concentration of Cu^{2+}. This trend is given up to a certain limit value of the concentration of Cu^{2+} ($[Cu^{2+}]_{lim}$), which increases with the increase of the solution temperature. At values greater than $[Cu^{2+}]_{lim}$, the concentration of all species produced in this stage of the process remain constant, and initiates the production of Cu^{2+} whose concentration increases linearly with increasing the initial Cu^{2+} concentration. From these results we can conclude that initial concentrations of Cu^{2+} less than 40 mM for solution temperatures around 60 °C and less than 50 mM for solution temperatures around 70 °C are adequate, because under these conditions all the Cu^{2+} is reduced to Cu^+. The $S_4O_6^{2-}$ produced is inert, thus not affecting the formation of sulfides of Cu and Sn; on the other hand, the species $S_2O_3^{2-}$ leads to the formation of HS^- ions, which acts as a source of S.

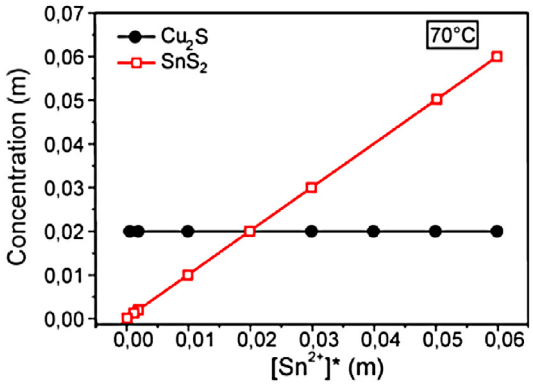

Fig. 4. Variation of the concentration of Cu_2S and SnS_2 as a function of the initial concentration of Sn^{2+}.

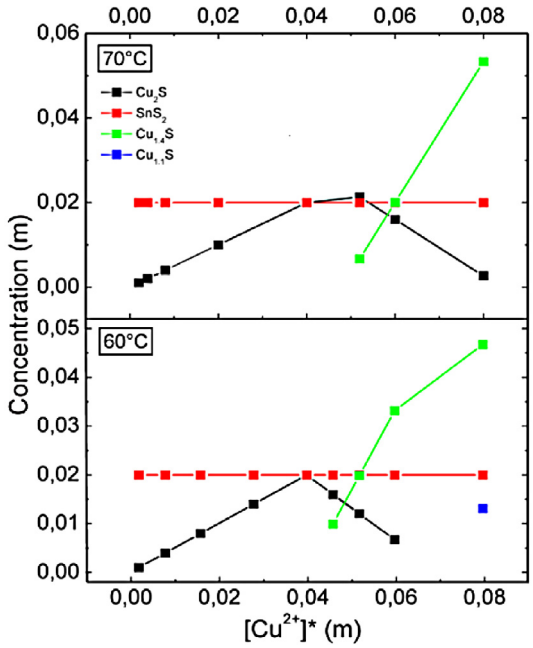

Fig. 5. Variation of the concentration of solid species (Cu_2S, SnS_2, $Cu_{1.4}S$ and $Cu_{1.1}S$) formed during the growth process as a function of the initial concentration of Cu^{2+}.

4.2 Formation of Cu_2S and SnS_2

Figure 4 shows the concentration of Cu_2S and SnS_2 as a function of the initial concentration of Sn^{2+} ($[Sn^{2+}]^*$), keeping the solution temperature at 70 °C and the $[Cu^{2+}]^*$ in 40 mM. This result indicates that the concentration of SnS_2 increases linearly with the increase of the initial concentration of Sn^{2+}, while the concentration of Cu_2S is not affected by the initial concentration of Sn^{2+}. It is also observed that when the initial concentration of Sn^{2+} is close to 20 mM, the production of SnS_2 tends to be approximately equal to that of Cu_2S.

Figure 5 shows curves of variation of the concentration of solid species formed during the growth process as a function of the initial concentration of Cu^{2+}, keeping $[Sn^{2+}]^*$ in 20 mM and the solution temperature at 60 and 70 °C respectively. In particular, the concentration of the solid species Cu_2S, SnS_2, $Cu_{1.4}S$ and $Cu_{1.1}S$ are plotted as function of the Cu^{2+} initial concentration. It can be observed that the concentration of SnS_2 remains constant with the increase of $[Cu^{2+}]^*$, while the concentration of the Cu_2S solid species increases linearly with the increase of $[Cu^{2+}]^*$. This trend is given up to a limit value $[Cu^{2+}]_{lim}$ of $[Cu^{2+}]^*$ of about 40 mM and 50 mM for a solution temperature of 60 °C and 70 °C respectively. At values greater than $[Cu^{2+}]_{lim}$, the concentration of Cu_2S decreases linearly with the increase of $[Cu^{2+}]^*$ and starts the formation of the $Cu_{1.4}S$ specie, whose concentration increases when $[Cu^{2+}]^*$ keeps on increasing. At values of $[Cu^{2+}]^*$ around 80 mM the solid specie $Cu_{1.1}S$ is additionally formed. It was also found that the concentration of the solid species formed increases slightly with an increase of the temperature from 60 to 70 °C. The calculations also revealed that the increase in temperature from 70 to 80 °C does not induce a significant change in the concentration of Cu_2S, SnS_2, $Cu_{1.4}S$ and $Cu_{1.1}S$ species. The formation of species different to Cu_2S derives from the temperature dependence of the reduction of Cu^{2+}, indicating that Cu^{2+} reduction is the main constraint on the formation of Cu_2S.

It was also found that the variation of the concentration of solid species formed as a function of a simultaneous variation of $[Cu^{2+}]^*$ and $[Sn^{2+}]^*$ maintaining a $[Cu^{2+}]^*/[Sn^{2+}]^*$ ratio of 2:1 and the solution temperature at 60 °C and 70 °C respectively, does not produce significant changes in the concentrations of solid species formed (Cu_2S, SnS_2, $Cu_{1.4}S$ and $Cu_{1.1}S$) as compared with those produced by varying only $[Cu^{2+}]^*$ or $[Sn^{2+}]^*$, indicating that the formation of SnS_2 and Cu_2S are independent of $[Cu^{2+}]^*$ and $[Sn^{2+}]^*$ respectively.

4.3 Cu_2SnS_3 formation

After studying the effect of the initial concentrations of Cu^{2+} and Sn^{2+} on the formation of the solid species Cu_2S and SnS_2 by solving the corresponding equilibrium equation using known values of the standard enthalpy of reaction ($\Delta_r H°$) and the equilibrium constant (K_{eq}), a simulation of the conditions to get the Cu_2SnS_3 compound was performed (Eq. (18)). As the equilibrium constant for the formation in aqueous media of the ternary compound has not been reported by other authors, we found an approximate value of K_{eq} corresponding to this reaction (Eq. (17)) by solving the equation of equilibrium assuming that K_{eq} is a variable parameter of the system

$$2Cu^{+} + Sn^{4+} + 3HS^{-} \rightarrow Cu_2SnS_3 + 3H^{+}. \qquad (18)$$

In Table 1 are listed values of concentration of the Cu_2S, SnS_2 and Cu_2SnS_3 compounds, calculated by varying $\log(K_{eq})$ between 80 and 100 and the synthesis temperature between 60 and 80 °C. For this study initial concentrations of Cu^{2+} and Sn^{2+} of 40 mM and 20 mM were used as well as a $[Cu^{2+}]^*/[Sn^{2+}]^*$ ratio of 2:1. The values of initial concentration of $S_2O_3^{2-}$ and Cit^{3-} were maintained as in the previous studies. The results show that

Table 1. Values of concentration of the Cu_2S, SnS_2 and Cu_2SnS_3 compounds estimated as a function of $\log(K_{eq})$ varying the temperature between 60 and 80 °C.

$\log(K_{eq})$	60 °C			70 °C			80 °C		
	concentration of solid species (m)								
	$[Cu_2SnS_3]$	$[Cu_2S]$	$[SnS_2]$	$[Cu_2SnS_3]$	$[Cu_2S]$	$[SnS_2]$	$[Cu_2SnS_3]$	$[Cu_2S]$	$[SnS_2]$
100	0.02			0.02			0.02		
90	0.0199		2.54×10^{-9}	0.0199		2.54×10^{-9}	0.0199		1.01×10^{-9}
80		0.02	0.02		0.02	0.02		0.02	0.02

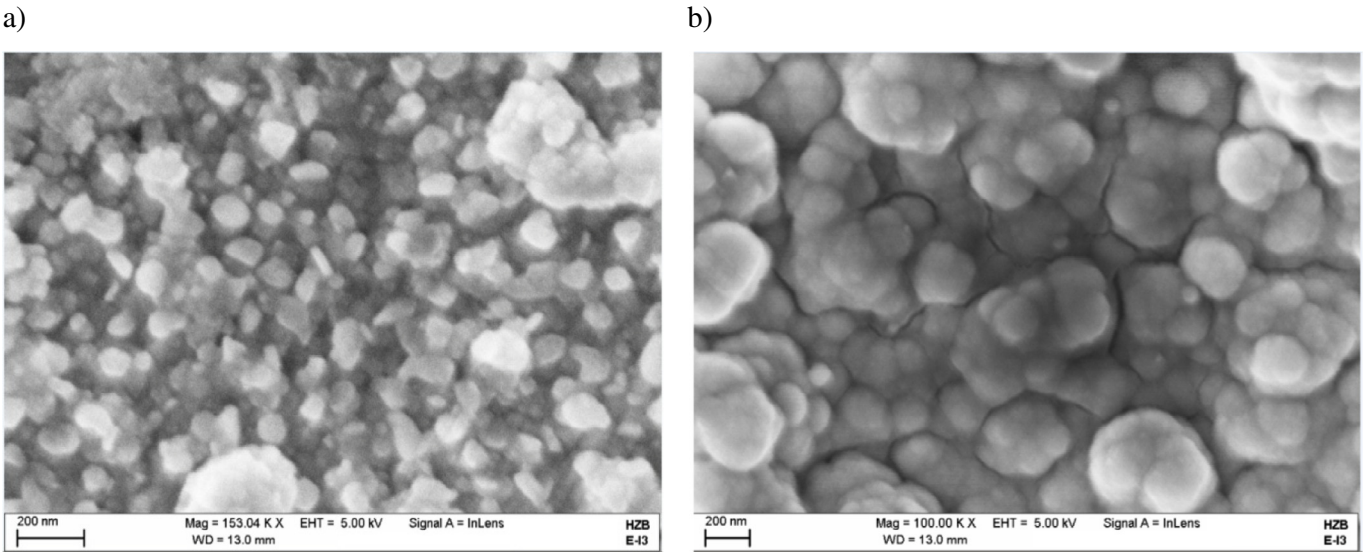

Fig. 6. Scanning Electron Microscopy (SEM) images of a typical thin film of (a) CTS and (b) CZTS deposited by membrane assisted CBD.

the formation of the compound Cu_2SnS_3 occurs at K_{eq} values in the range of 10^{90}–10^{100}. Below these values the simulation predicts a mixture of secondary solid phases instead the desired compound.

4.4 Morphological characterization

Figure 6 shows SEM micrograph (top view) of CTS and CZTS thin films prepared under the conditions that gave rise to the manufacture of the highest efficiency solar cells; it is observed that in general, the CTS and CZTS films consist of compact grain structures with sub-micron size. CZTS films tend to grow with grains grouped together in big clusters of different size, while the CTS samples show small grains with presence of some voids and some small clusters. From the SEM images shown in Figure 6 was found that the average size of the crystallites of CZTS thin films is around 176 ± 40 nm and that of the CTS samples is of the order of 107 ± 17 nm. The grain size of the CZTS films prepared in this work is significantly smaller than the reported for CZTS films deposited by evaporation [21] and by spin coating from a hydrazine based solution [22] which grow with micrometer-sized grains. Considering that large grains generally benefit device performance because of less opportunity for recombination of photogenerated carriers at the grain boundaries, it would convenient to increase its grain size which could be achieved by optimizing the post-deposition annealing and/or through a refinement of the growth kinetics to favor the heterogeneous growth.

4.5 Experimental verification of the formation of the Cu_2SnS_3 and Cu_2SnS_4 compounds

Using as reference the parameters values determined theoretically as described above, a parameter study was done for finding suitable conditions to grow thin films of Cu_2SnS_3 from co-precipitation of Cu_2S and SnS_2. The following chemical bath composition leaded to the growth of Cu_2SnS_3 thin films: $[CuCl_2] = 20$ mM, $[SnCl_2] = 60$ mM, $[Na_2S_2O_3] = 250$ mM, $[Na_3C_6H_5O_7] = 237$ mM, bath temperature of 70 °C; the pH of the working solution at the beginning of the co-precipitation process is about 5.8, but this value decreases during the process, so that at the end it reach a value of around 5. The experimental values of synthesis parameters that leaded the growth of Cu_2SnS_3 films reasonably match with those estimated through the theoretical simulation; a concentration of $SnCl_2$ greater than that estimated theoretically to get a stoichiometric compound was used to compensate the loss of Sn that occurs during post annealing at 550 °C performed to obtain Cu_2SnS_3 thin films with improved crystalline structure.

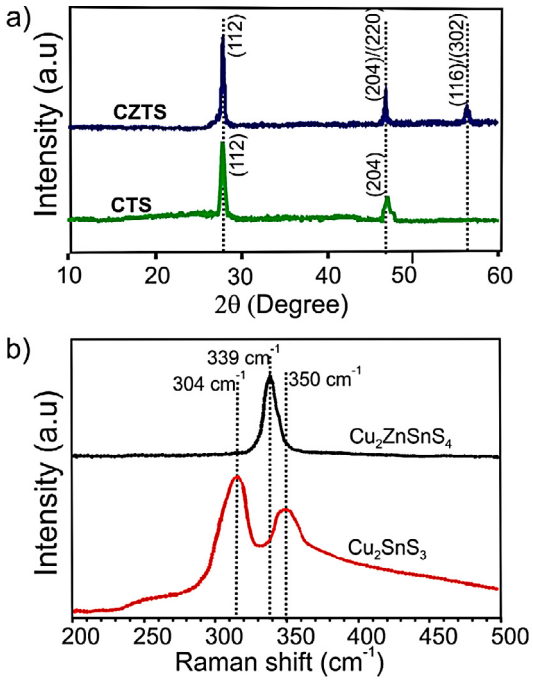

Fig. 7. (a) XRD pattern, (b) Raman spectra of typical thin films of CTZ and CZTS.

In Figure 7a are shown typical XRD spectra corresponding to both Cu_2SnS_3 and Cu_2ZnSnS_4 thin films. From the XRD pattern obtained for the CTS sample, it can be observed the presence of reflections along the planes (112), (204) that have been assigned to the Cu_2SnS_3 phase with a tetragonal structure (ICDD data file # 01-089-4714) [23]. The XRD patterns of the CZTS thin film exhibit Bragg peaks of (112), (204/220), (116/312) that according to the JCPDS data file # 26-0575 can be assigned to the diffraction lines of CZTS with a kesterite structure [24].

The comparison between the diffractogram of the CZTS film and the CTS film, allows to conclude that these two diffractograms differ very little from each other. This result indicates that the XRD measurements cannot precisely determine whether the observed reflections correspond to Cu_2ZnSnS_4 or Cu_2SnS_3 and thus the use of a complementary technique is needed.

In Figure 7b are depicted typical Raman spectra of both CZTS and CTS films. The CZTS sample exhibits a dominant peak located around 339 cm^{-1}, which has been attributed to the Cu_2ZnSnS_4 phase [21]; considering that this peak is quite narrow it could be argued that there is no clear evidence of the formation of secondary phases. The CTS film exhibit Raman peaks at 304 and 350 cm^{-1}; these peaks have been assigned by other authors to the A′ symmetry vibrational modes from the tetragonal Cu_2SnS_3 phase [23–26], indicating that the method developed, allows to grow thin films containing only the Cu_2SnS_3 phase.

In an article published previously [13] there were reported results of a study performed using XRD, Raman spectroscopy and XPS (X-ray photoelectron spectroscopy) to thin films of CTS and CZTS deposited by both membrane assisted CBD and sequential evaporation of precursors. The XRD and Raman study revealed that with both methods can be grown samples of CTS containing just the Cu_2SnS_3 phase and samples of CZTS containing only the Cu_2ZnSnS_4 phase; it was also reported that the CBD deposited CTS and CZTS films present similar structural properties than those of the sequentially evaporated CTS and CZTS films. On the other hand, from the XPS results was found that in both types of compounds copper is in the +1 oxidation state and S is in the −2 oxidation state; these results also confirm the valence (IV) for Sn. The XPS spectrum of the CZTS films exhibit additionally peaks corresponding to $Zn2p_{3/2}$ and $Zn2p_{1/2}$ visible at binding energy of 1021.8 and 1044.6 eV with a peak separation of 22.8 eV in, indicating that Zn is in the +2 oxidation state. XPS depth profile analysis performed to Cu_2ZnSnS_4 and Cu_2SnS_3 films (see Ref. [13]) do not revealed the presence of oxygen; nevertheless peaks associated to C1s were also identified.

The analysis XPS realized to the samples of CTS and CZTS synthesized in this work reveal that these grow predominantly in the phases Cu_2SnS_3 and Cu_2ZnSnS_4, result that agrees with the obtained from XRD and Raman spectroscopy measurements.

4.6 Performance of Mo/Cu_2ZnSnS_4/Zn(S,O)/ i-ZnO/n^+-ZnO solar cells

Solar cells with structure Mo/Cu_2ZnSnS_4/Zn(S,O)/ i-ZnO/n^+-ZnO were fabricated and the J-V characteristic was measured under AM 1.5 irradiance (100 mW/cm^2) after light soaking for 8 min. Typically, the cells were fabricated using a 2.5 μm thick CZTS film, a 60 nm thick ZnS buffer layer deposited by CBD, a 30 nm thick i-ZnO layer and a 0.8 μm thick n^+-ZnO layer; the i-ZnO and n^+-ZnO layers were deposited in situ by reactive evaporation (see details in Ref. [27]). In Figure 8a is displayed the J-V curve of the best solar cell presenting $\eta = 4.2\%$ with open-circuit voltage (V_{OC}) = 0.495 V, short-circuit current density (J_{sc}) = 16.2 mA/cm^2, fill factor (FF) = 0.54. The active area of this device was 1.0 cm^2. To gain further insights in the device performance and loss mechanisms the external quantum efficiency (EQE) was measured on the same solar cell as shown in Figure 8b.

The EQE data has a weak decay in the long wavelength region. Usually, this weak decay is interpreted as a short minority carrier diffusion length, which lead to a reduced collection efficiency of photo-carriers created deep in the absorber. The small values of the diffusion length could be related with small values of grain size of the CZTS and also to high densities of states associated with traps and centers of recombination generated by imperfections of the crystal lattice or by natives defects. It is clear from Figure 8b that the EQE of the cells is quite low in the region of wavelengths lower than 500 nm; this behavior could be attributed to loss of photocurrent caused by recombination of photo-carriers in surface states of the CZTS absorber layer.

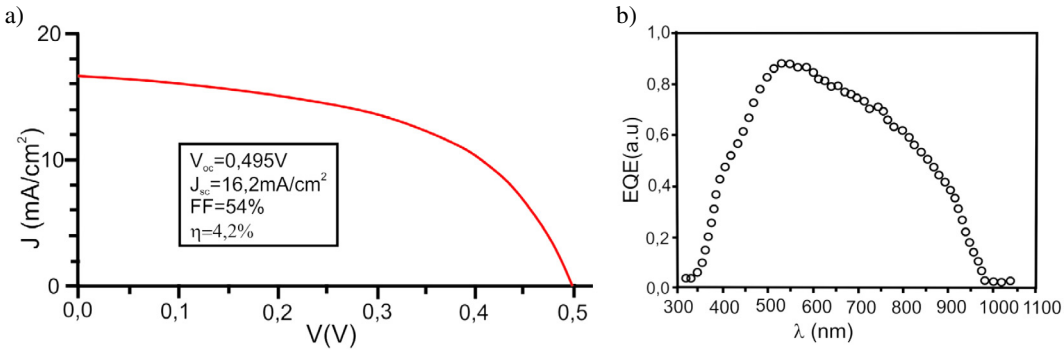

Fig. 8. (a) *J-V* curve and (b) external quantum efficiency of the best performance solar cell.

Table 2. Device characteristics of the performance of five CZTS cells fabricated varying the thickness and resistivity of the CZTS layer.

d(CZTS) μm	ρ (CZTS) (Ω cm)	η (%)	FF (%)	V_{oc} (mV)	J_{sc} (mA/cm^2)
1.6	40.7	3.3	46	475	15.1
2.3	1015	3.3	45	485	15.0
2.5	38.4	4.2	54	495	16.2
2.6	3.5	3.9	51	483	16.0
3.4	42.6	3.6	49	463	15.9

In Table 2 are presented device characteristics of five solar cells (cells C1-C5) fabricated varying the thickness d and the resistivity ρ of the CZTS layer. The resistivity was varied by varying the composition ([Cu/(Zn+Sn)]) ratio of the precursor solution, keeping constant a Zn rich Zn/Sn ratio.

From the data in Table 2, it is observed that the low efficiency of CZTS devices is mainly caused by poor *FF* and low short circuit current (J_{sc}). Considering that the *FF* depends on the diode quality factor β as well as of effects of both series and shunt resistances, the high values of the series resistance (which has relation with the resistivity ρ of the cells) could be one of the causes of the low value of *FF*. On the other hand, taken into account that the diode quality factor is affected by recombination through trap centers inside the depletion region [28], can be considered that additional losses of the *FF* are related with a high density of recombination centres in the depletion layer of the device.

The low values of J_{sc} of the cells fabricated in this work, suggest low collection of the photo-generated carriers which can be attributed to factors such as, short minority carrier diffusion length related with the small values of grain size of the CZTS films and also to high densities of states associated with traps and centers of recombination. High recombination in states of interface, may be another factor that contributes to the losses of the short circuit current.

The best efficiency obtained in this work (4.2%) is significantly inferior than the highest efficiency reported currently for this type of cells fabricated by vacuum deposition process (8.4%) [21]; however bearing in mind that in this work preliminary results are presented, the performance of the cells could be improved by refining the growth process of the CZTS films through a better control of the kinetics of growth and optimizing the parameters of synthesis. The performance of the devices could also be improved increasing the grain size of the CZTS films, which could be achieved by optimizing the post-deposition annealing.

5 Conclusions

A novel procedure for growing single phase Cu_2ZnSnS_4 (CZTS) thin films using a solution-based chemical route was presented. This consist in sequential deposition of Cu_2SnS_3 (CTS) and Zn(S,O) thin films followed by annealing at 550 °C in nitrogen atmosphere, where the CTS compound is prepared in one step process by simultaneous precipitation of Cu_2S and SnS_2 performed by diffusion membranes assisted CBD technique.

As the conditions in terms of concentration of metal species, sulphide anion and temperature required for the formation of the Cu_2SnS_3 compound have not yet been reported by other authors, these were obtained solving the equilibrium equation of the system $SnCl_2$, $Na_3C_6H_5O_7{\cdot}2H_2O$, $CuCl_2$ and $Na_2S_2O_3{\cdot}5H_2O$ with the help of the Visual MINTEQ 3.0 package, supported on the program MINTEQA2. Taking as reference these results, a parameter study was done to achieve experimental conditions to prepare Cu_2SnS_3 and Cu_2ZnSnS_4 films free of secondary phases. The following chemical bath composition leaded to the growth of single phase Cu_2SnS_3 films: $[CuCl_2]$ = 20 mM, $[SnCl_2]$ = 60 mM, $[Na_2S_2O_3]$ = 250 mM, $[Na_3C_6H_5O_7]$ = 237 mM, bath temperature of 70 °C and final pH around 5. The experimental values of synthesis parameters which allowed to grow Cu_2SnS_3 films reasonably match with those estimated through the theoretical simulation. Single phase Cu_2ZnSnS_4 thin films were achieved from CTS and Zn(S,O) thin films sequentially deposited by membrane assisted CBD and conventional CBD methods respectively. X-ray diffraction and Raman spectroscopy measurements confirmed the growth of Cu_2SnS_3 and Cu_2ZnSnS_4 films free of secondary phases. The main advantage of the membrane assisted

CBD method respect to the conventional CBD, lies in the fact that the first one favors the heterogeneous growth which contributes to prevent the formation of clusters, as a result of the physical barrier provided by the membrane.

The applicability for solar cells of the CZTS films prepared using a novel solution based route was demonstrated. Efficiencies of 4.2% were achieved with solar cells fabricated with structure $Mo/Cu_2ZnSnS_4/ZnS/i\text{-}ZnO/n^+\text{-}ZnO$.

This work was supported by Colciencias (Contract # 038/2013) and Universidad Nacional de Colombia, Sede Bogotá, Facultad de Ciencias, Grupo GMS&ES, Bogotá DC, Colombia (Proy. 28135 supported by DIB). The authors would like to thank the Helmholtz Zentrum Berlin for its cooperation with the SEM and XPS measurements.

References

1. Solar Frontier Press Release. Solar frontier achieves world record thin-film solar cell efficiency: 22.3%, 8 December 2015 http://www.solar-frontier.eu/uploads/media/SFE-Thin-Film-Solar-Cell-Efficiency-EN.pdf
2. K. Wang, O. Gunawan, T. Todorov, B. Shin, S.J. Chey, N.A. Bojarczuk, D. Mitzi, S. Guha, Appl. Phys. Lett. **97**, 143508 (2010)
3. H. Katagiri, K. Jimbo, S. Yamada, T. Kamimura, W.S. Maw, T. Fukano, T. Ito, T. Motohiro, Appl. Phys. Express **1**, 41201 (2008)
4. D.A.R. Barkhouse, O. Gunawan, T. Gokmen, T.K. Todorov, D.B. Mitzi, Progr. Photovolt.: Res. Appl. **20**, 6 (2012)
5. T.K. Todorov, J. Tang, S. Bag, O. Gunawan, T. Gokmen, Y. Zhu, D.B. Mitzi, Adv. Ener. Mater. **3**, 34 (2013)
6. A.S. Ionkin, B.M. Fish, W.J. Marshall, R.H. Senigo, Solar Ener. Mater. Solar Cells **104**, 23 (2012)
7. P.A. Fernandes, P.M.P. Salomé, A.F. da Cunha, J. Alloys Compd. **509**, 76000 (2011)
8. H. Araki, A. Mikaduki, Y. Kubo, T. Sato, K. Jimbo, W.S. Maw, H. Katagiri, M. Yamazaki, K. Oishi, A. Takeuchi, Thin Solid Films **517**, 1457 (2008)
9. Y. Li, T. Yuan, L. Jiang, F. Liu, Y. Liu, Y. Lai, J. Mater. Sci.: Mater. Electron. **26**, 204 (2015)
10. C. Gougaud, D. Rai, S. Delbos, E. Chassaing, D. Lincot, J. Electrochem. Soc. **160**, D485 (2013)
11. K. Jimbo, R. Kimura, T. Kamimura, S. Yamada, W.S. Maw, H. Araki, K. Oishi, H. Katagiri, Thin Solid Films **515**, 5997 (2007)
12. J. Kim, H. Hiroi, T.K. Todorov, O. Gunawan, M. Kuwahara, T. Gokmen, D. Nair, M. Hopstaken, B. Shin, Y.S. Lee, W. Wang, H. Sugimoto, D.B. Mitzi, Adv. Mater. **26**, 7427 (2014)
13. C. Calderón, G. Gordillo, R. Becerra, P. Bartolo-Pérez, Mater. Sci. Semicond. Processing **39**, 492 (2015)
14. G. Hodes, *Chemical solution deposition of semiconductor films* (Marcel Dekker Inc., New York, 2002)
15. N. Naghavi, D. Abou-Ras, N. Allsop, N. Barreau, S. Bucheler, A. Ennaoui, C.-H. Fischer, C. Guillen, D. Hariskos, J. Herrero, R. Klenk, K. Kushiya, D. Lincot, R. Menner, T. Nakada, C. Platzer-Björkman, S. Spiering, A.N. Tiwari, T. Törndahl, Prog. Photovolt: Res. Appl. **18**, 411 (2010)
16. U. Gangopadhyay, Kyunghae Kim, D. Mangalaraj, Junsin Yi, Appl. Surf. Sci. **230**, 364 (2004)
17. C. Gao, H. Shen, Thin Solid Films **520**, 3523 (2012)
18. I. Grozdanov, C.K. Barlingaya, S.K. Dey, M. Ristov, M. Najdoski, Thin Solid Films **250**, 67 (1994)
19. C. Han, Q. Liu, D.G. Ivey, Electrochimica Acta **53**, 8332 (2008)
20. H. Guan, H. Shen, C. Gao, X. He, J. Mater. Sci.: Mater. Electron. **24**, 1490 (2013)
21. B. Shin, O. Gunawan, Y. Zhu, N.A. Bojarczuk, S.J. Che, S. Guha, Prog. Photovolt: Res. Appl. **21**, 72 (2013)
22. T.K. Todorov, K.B. Reuter, D.B. Mitzi, Adv. Mater. **22**, 1 (2010)
23. P.A. Fernandes, P.M.P. Salomeand, A.F. da Cunha, J. Phys. D **43**, 215403 (2010)
24. T. Tanaka, A. Yoshida, D. Saiki, K. Saito, Q. Guo, M. Nishio, T. Yamaguchi, Thin Solid Films **518**, S29 (2010)
25. M. Altosaar, J. Raudoja, K. Timmo, M. Danilson, M. Grossberg, J. Krustok, E. Mellikov, Phys. Status Solidi A **205**, 167 (2008)
26. X. Lin, J. Kavalakkatt, K. Kornhuber, S. Levcenko, M.Ch. Lux-Steiner, A. Ennaoui, Thin Solid Films **535**, 10 (2013)
27. J.S. Oyola, J.M. Castro, G. Gordillo, Solar Energy Mater. Solar Cells **102**, 137 (2012)
28. P. Mialhe, J.P. Charles, A. Khoury, G. Bordure, J. Phys. D **19**, 483 (1986)

Cite this article as: John M. Correa, Raúl A. Becerra, Asdrubal A. Ramírez, Gerardo Gordillo, Fabrication of solar cells based on Cu_2ZnSnS_4 prepared from Cu_2SnS_3 synthesized using a novel chemical procedure, EPJ Photovoltaics **7**, 70305 (2016).